Synthetic Metals 253 (2019) 122–130

Contents lists available at ScienceDirect

Synthetic Metals

journal homepage: www.elsevier.com/locate/synmet

Effects of carbon nanotube on the thermal, mechanical, and electrical properties of PLA/CNT printed parts in the FDM process

Leipeng Yang[a], Shujuan Li[a,*], Xing Zhou[b], Jia Liu[a], Yan Li[a], Mingshun Yang[a], Qilong Yuan[a], Wei Zhang[b]

[a] School of Mechanical and Precision Instrument Engineering, Xi'an University of Technology, Xi'an 710048, PR China
[b] Faculty of Printing, Packaging Engineering and Digital Media Technology, Xi'an University of Technology, Xi'an 710048, PR China

ARTICLE INFO

Keywords:
Fused deposition modeling
Carbon nanotubes
Electrical property
Mechanical property

ABSTRACT

In this work, a filament based on polylactic acid (PLA)/ carbon nanotube (CNT) composites was prepared for the fused deposition modeling (FDM) process. The effects of the CNT content on the crystallization-melting behavior and melt flow rate (MFR) were tested to research the printability of the PLA/CNT. The results demonstrate that the CNT content has a significant influence on the mechanical properties and conductivity properties. The addition of 6 wt% CNT produced a 64.12% increase in tensile strength and a 29.29% increase in flexural strength. The electrical resistivity varied from approximately 1×10^{12} Ω/sq to 1×10^{2} Ω/sq for CNT contents ranging from 0 wt% to 8 wt%. In addition, this paper assesses the effect of the filling velocity, liquefier temperature and layer thickness on the electrical resistivity. A lower filling velocity, higher liquefier temperature and greater layer thickness should be selected to achieve excellent electrical conductivity. These results demonstrate that PLA/CNT composites are a promising functionalizing material for FDM.

1. Introduction

As one of the most promising 3D printing technologies, FDM shows high potential for application, including but not limited to functional testing, design verification and medical applications [1]. As a filament-based and thermally driven process, the polymer filaments are inserted into a heated nozzle and melted. The nozzle moves and extrudes a semimolten polymer onto a substrate or previously deposited layers to fabricate the desired 3D components directly. Owing to the microstructural anisotropy and the layer-by-layer effect of the forming process, the mechanical behaviors and the fabrication qualities of the finished part formed by the FDM process are poorer than those of the finished part formed by conventional manufacturing techniques. Two kinds of methods to conquer this restriction have been recommended [2,3].

The first method is to strengthen the mechanical properties and manufacturing qualities based on adjustment and optimization of the process parameters. Sood et al. [4] conducted experiments based on central composite design (CCD) and established a functional relationship between process parameters and strength. The validity of the models was tested using analysis of variance (ANOVA). Rayegani et al. [5] adopted a method of full factorial design, the group method of data handling (GMDH) and differential evolution (DE) and also proposed that the build orientation, air gap, wire-width compensation and raster angle affect the tensile strength of FDM-fabricated parts. The optimum process parameters to achieve the ultimate tensile strength were acquired. Peng et al. [6] used response surface methodology (RSM) combined with a fuzzy inference system (FIS) to look into the results of parameters such as the extrusion speed, width, layer thickness, and filling speed on the manufacturing accuracy and efficiency. Dawoud et al. [7] suggested that the proper setting of FDM parameters can achieve the same mechanical properties as those parts formed by traditional processing methods. Torres et al. [8] reported the effect of several key parameters on the mechanical performance of FDM-processed prototypes. As a result, a slower speed and lower layer thickness were found to lead to an elevated surface quality. Panda et al. [9] posed a challenging multi-objective optimization research query about the fabrication accuracy and quality by employing an evolutionary system identification method, and the subsequent study showed that the layer thickness and extrusion speed influence the warpage. In addition, the filling speed and line-width interpolation were found to influence the dimension error the most. Singh [10] researched and optimized the process variables of single-screw extruder formed 3D-parts; functional relationships of the tensile strength, modulus of elasticity and error

* Corresponding author.
E-mail address: shujuanli@xaut.edu.cn (S. Li).

https://doi.org/10.1016/j.synthmet.2019.05.008
Received 17 December 2018; Received in revised form 12 April 2019; Accepted 16 May 2019

were also created, and adequate selections of screw extruder technological variables were acquired. Mohamed [11] established functional relations to predict the processing time, materials cost and mechanical behavior and identified the most influential parameters, including the air gap, layer thickness and build direction. Vahabli [12] designed a specific test-piece to predict the surface quality distribution for variable raster angles based on the radial basis function neural network-imperialist competitive algorithm (RBFNN-ICA) model.

The second method to obtain excellent mechanical performance is to exploit new materials with appropriate thermal and rheological properties. Jia et al. [13] incorporated POE-g-MAH and PS into PA6 to prepare a new type of PA6-based polymer composite with excellent toughness for FDM. Ning et al. [14] added carbon fibers into ABS to form thermoplastic matrix carbon fiber reinforced plastic (CFRP) composites to improve the mechanical performance of the FDM prototype. Chen et al. [15] demonstrated the FDM fabrication of TPU/PLA/GO composites and their possible applications as biocompatible materials. Zhang et al. [16] reported the 3D printing of the soft-printing circuit on the basis of a mixture of PLA and r-GO through a melting blend. Yu et al. [3] prepared a filament of PLA/graphene nanofiller composites for the FDM process and found that the electric conductivities of the PLA-matrix composites increased. Postiglione et al. [17] developed new 3D-printing equipment on the basis of liquid deposition modeling to fabricate electric PLA/MWCNT-based composite microstructures. Zhu et al. [18] prepared ABS/SAN composites with different proportions for the FDM forming process, and the performance of ABS was found to be improved with SAN. Tian et al. [19] proposed a new 3D-printing system to fabricate reinforced thermoplastic composite-based infinite fibers, which employed infinite carbon fibers and PLA as the reinforcing and matrix phases, respectively. Wang et al. [20] prepared PCL/Nd-Fe-B composites for the FDM forming process and proposed a new method to achieve an antigravitational printing process. Barrau S et al. [21] dispersed the CNT in an ABS matrix to achieve improved mechanical properties, electrical conductivity and thermal stability in the FDM process.

Although some tentative studies on different reinforcement polymer composites have been performed to improve the properties of FDM-processed parts, the influence of carbon on the thermal, mechanical, and electrical properties of PLA/CNT-prepared filament has not been systematically reported. In addition, there are no reported experimental investigations on the effect of the process parameters on the electrical properties of the final printed PLA/CNT parts. On the basis of these considerations, PLA/CNT composites were prepared by melting blend, and the effects of the CNT content on the crystallization-melting behavior and MFR were investigated. On this basis, the mechanical properties and electrical conductivity of PLA/CNT blends for FDM parts were studied. In addition, the fracture interface of tensile specimens and the surface morphology of electrical resistivity testing specimens at each CNT content level were observed using SEM to analyze the specimen fracture and electrical conductivity mechanisms. Furthermore, process parameters, such as the filling velocity, liquefier temperature, and layer thickness, were investigated and optimized in light of their effect on the electrical resistivity of the FDM parts. Composite parts with excellent electrical conductivity were formed to validate the practicability of the recommended FDM 3D-printing process based on optimized process parameters.

2. Experiment

2.1. Preparation of PLA/CNT blend filaments

A mixture of the PLA pellets (3052D, NatureWorks LLC) and CNT (diameter: 13 nm, length: 10 μm, Tanfeng Graphene Technology Co., Ltd., Suzhou, China) was obtained by a blender with different CNT contents (0 wt%, 2 wt%, 4 wt%, 6 wt% and 8 wt%). After drying at 80 °C for 8 h, the PLA/CNT composites were obtained using a double screw extruder (Hone Machinery & Electronics Co., Ltd., Nanjing, China), with a screw length to diameter ratio of 40/1. The temperature distribution during extrusion was 165 °C, 175 °C, 175 °C, 180 °C, 180 °C, 180 °C, 185 °C, and 185 °C, and the head was 180 °C. The screw speed and feed speed were set as 15 r/min and 10 r/min, respectively. The extruded strands of the PLA/CNT composites were water-cooled, granulated, and dried before further processes. Then, a Wellzoom-C single screw extruder (Mistar Technology Co., Ltd., Shenzhen, China) was employed to prepare the filaments for the FDM forming process (diameter: 1.75 ± 0.1 mm) with the as-prepared granules. The preheating temperature and extrusion head temperature were 205 °C and 220 °C, respectively.

Table 1
The values of the fixed factors.

Fixed parameters	Value	Unit
Build orientation	0	deg
Filament diameter	1.75	mm
Ambient temperature	50	°C
Air gap	0	mm
Filling rate	100	%
Part filling style	Perimeter/raster	–
Number of contours	5	–

Table 2
The controllable factors and levels.

Factor	Symbol	Level			Unit
		Low (-1)	Center (0)	High (1)	
Filling velocity	A	20	40	60	mm/s
Liquefier temperature	B	200	215	230	°C
Layer thickness	C	0.1	0.2	0.3	mm

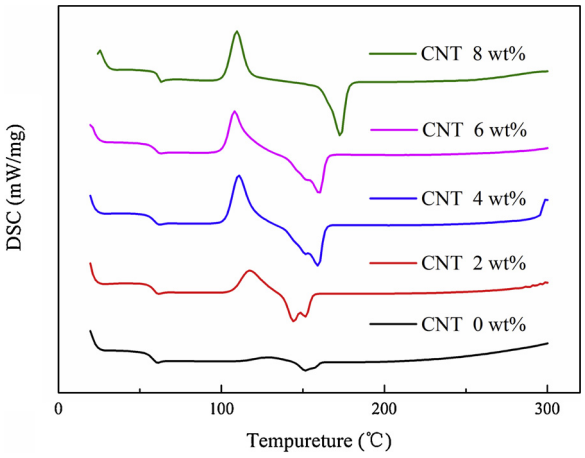

Fig. 1. The DSC curves of filaments with different CNT contents.

Table 3
Effects of the CNT content on the thermal properties of PLA/CNT.

	T_g/°C	T_{cc}/°C	T_m/°C
CNT 0 wt%	56.98	N/A	151.09
CNT 2 wt%	57.81	117.55	151.92
CNT 4 wt%	58.23	111.50	159.14
CNT 6 wt%	59.81	108.68	160.38
CNT 8 wt%	61.04	109.92	172.48

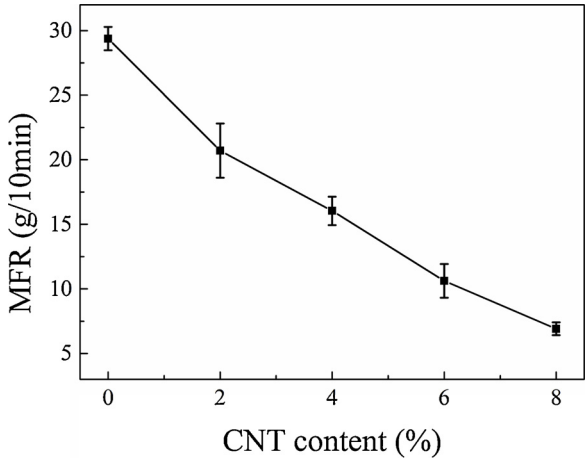

Fig. 2. Effects of the CNT content on the MFR of PLA/CNT blends.

2.2. FDM printer and settings

All test specimens were formed by employing a Raise3D N2 Plus 3D printer (Raise3D, Inc., Shanghai, China) in this work. During the FDM process, the nozzle diameter, liquefier temperature, filling velocity and layer thickness were set at 0.8 mm, 215 °C, 50 mm/s and 0.2 mm, respectively. Table 1 shows the other fixed parameters.

In order to study the effects of the CNT content on both the mechanical properties and electrical conductivity of FDM-printed specimens, three kinds of specimens were prepared for each parameter. The tensile specimens and the flexural specimens were prepared and tested based on ISO 527:2012 and ISO 178:2010 standards, respectively. To perform electrical resistivity testing, 15 mm × 15 mm × 2 mm samples were prepared by the FDM process. In addition, to investigate the impact of technological variables on the electrical conductivity of specimens, each variable was studied over an extended range, as shown in Table 2.

2.3. Measurement procedures

The crystallization-melting behaviors of the PLA/CNT composites were obtained by employing a DSC 200 F3 (NETZSCH-Geratebau GmbH, German). Measurements were implemented with approximately 6 mg samples, which were first heated from 20 °C to 300 °C at a rate of 20 °C/min and kept at 300 °C for 1 min to reset the thermal history. Then, the samples were cooled at a rate of 10 °C/min to 20 °C and kept at 20 °C for 1 min. Subsequently, the samples were reheated from 20 °C to 300 °C at a rate of 10 °C/min. Some physical quantities can be obtained from the melting curves of the second heating step, including the glass transition temperature (T_g), melting temperature (T_m), and cold crystallization temperature (T_{cc}). The MFR of the PLA/CNT composites was tested using an XNR-400A melt flow rate tester (Dingsheng Tester Detection Equipment Co., Ltd., Chengde, China) according to the ISO 1133:2011 standard. An XWW-10 universal mechanical tester (Jiezhun Instrument Equipment Co., Ltd., Shanghai, China) was employed for tensile and flexural testing, which was performed at 10 mm/min and 2 mm/min, respectively. The mechanical behavior of the PLA/CNT parts was measured five times by testing five specimens at each CNT content level. The electrical resistivity of the PLA/CNT samples was measured by using an RTS-9 four point probe meter (Four Probe Technology Co., Ltd., Guangzhou, China) and SM7110 super megohmmeter (Hioki E. E. Co., Japan) for lower ($\leq 10^4$ Ω/sq) and higher ($> 10^4$ Ω/sq) electrical resistivity, respectively. The average of five measurements represents the resistivity value of each sample. An SU 8010 SEM (Hitachi Co., Tokyo, Japan) was employed to observe the fracture interface of the mechanical testing specimens and surface morphology of the electrical resistivity testing specimens at different

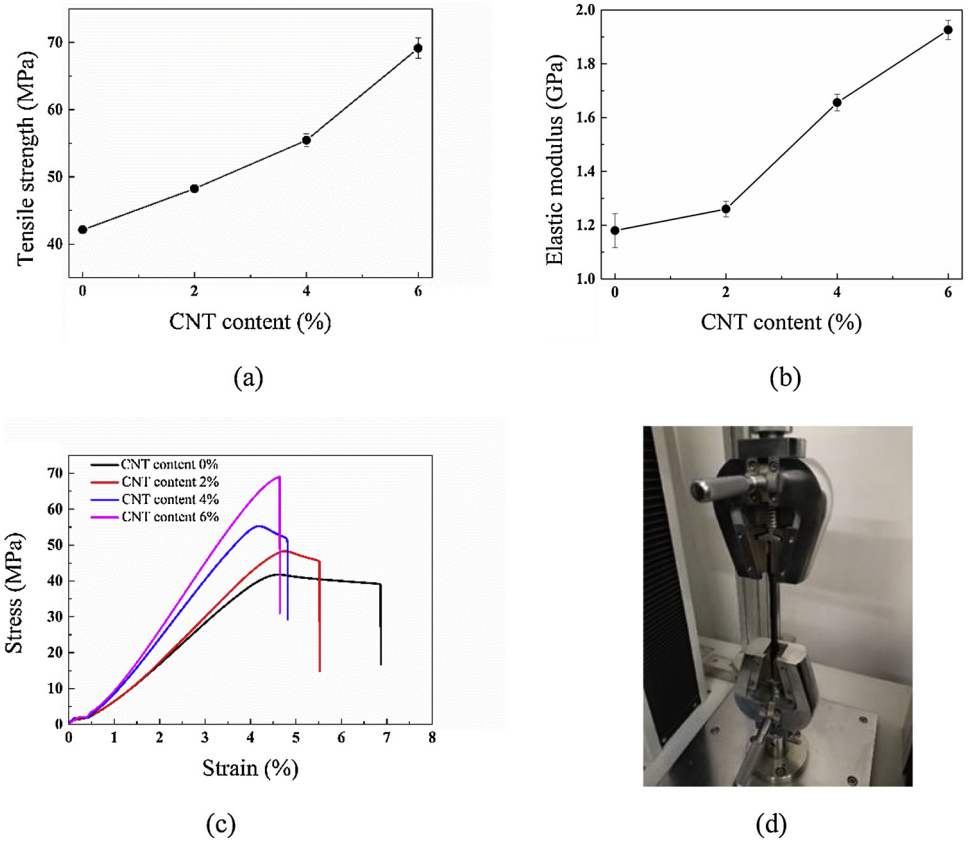

Fig. 3. Effects of the CNT content on the (a) tensile strength, (b) elastic modulus, and (c) representative stress-strain curves and (d) tensile test diagram.

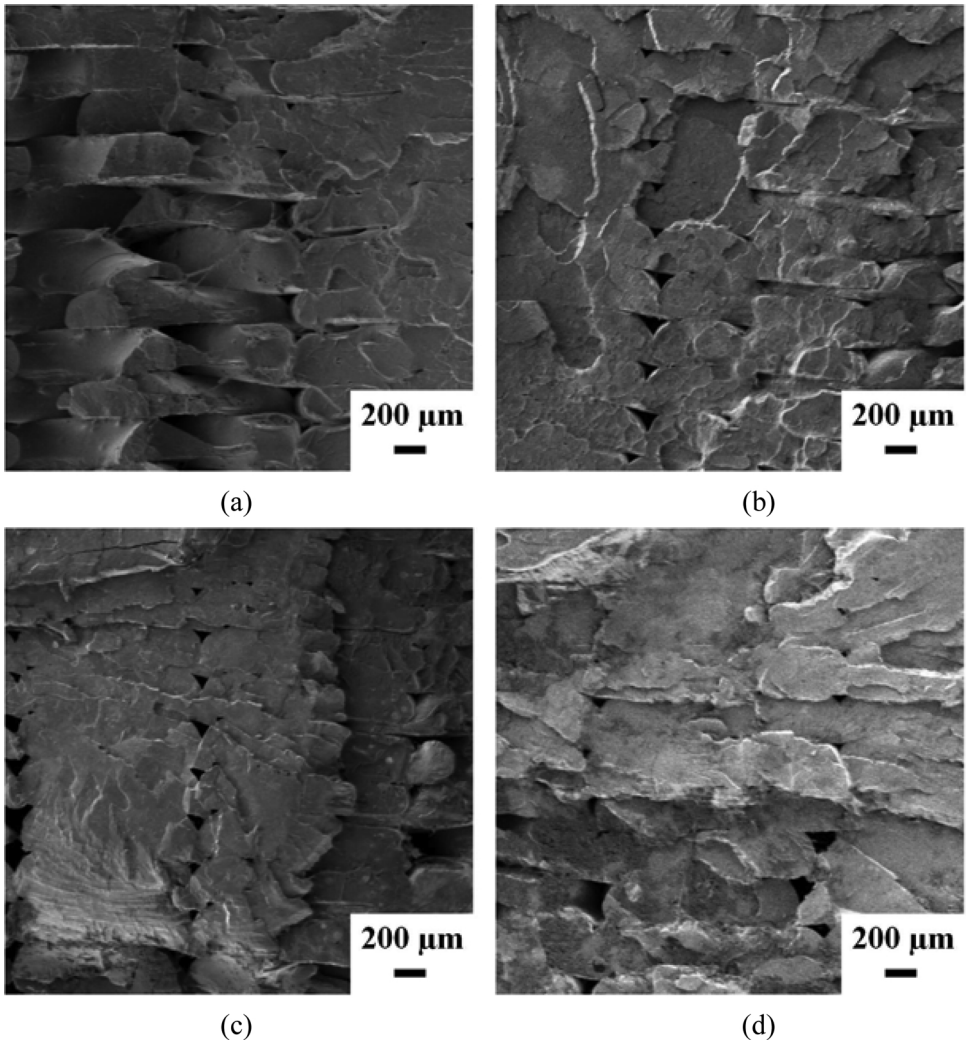

Fig. 4. The SEM fracture interface of specimens with (a) 0 wt%, (b) 2 wt%, (c) 4 wt% and (d) 6 wt% CNT content.

magnifications.

3. Results and discussion

3.1. Crystallization-melting behavior and rheological properties

3.1.1. Effects of the CNT content on the crystallization-melting behavior

Fig. 1 shows the representative DSC curves of composites with different CNT content. The T_g, T_{cc} and T_m of different samples are easily obtained from the DSC curves. As shown in Table 3, the T_g of PLA and PLA/8 wt% CNT were approximately 56.98 ℃ and 61.04 ℃, respectively. The results are consistent with previous reports [22,23]. The analysis is complicated by the fact that the glass transition is affected by many factors, such as the branched structure, steric effects, chain flexibility, crosslinking, molecular weight and interactions. The T_g of the PLA/CNT composites tends to increase with the addition of CNTs, possibly due to the interactions between the PLA and the CNT, which causes the reduction of molecular flexibility and chain mobility at the zone surrounding the carbon nanotubes. Moreover, formative physical crosslinking could result in the reduction of the free volume in the polymer composites. The T_m of PLA was approximately 151.09 ℃, whereas in the composites, a marginal increase was obtained with the addition of CNT. Consequently, the PLA/8 wt% CNT composite presented a melting point at 172.48 ℃. The same phenomena can be found in a previous research [23], in which T_m increased with additional CNT content due to the nucleation effect by nanoparticles. It can also be validated that the fusion heat values of composites are higher than the corresponding values of pure PLA. The T_{cc} measurements clearly demonstrated the nucleating effect of the CNT on the PLA crystallization behavior. The T_{cc} values of the PLA/CNT composites were lower than that of pure PLA. For instance, T_{cc} decreased from 117.55 ℃ for PLA/2 wt% CNT to 109.92 ℃ for PLA/8 wt% CNT. The decrease in T_{cc} values demonstrated that cold crystallization in the composites is more spontaneous than that in pure PLA because the CNT strengthen the crystallization of PLA, acting as a nucleator. All of these results demonstrate that the addition of CNT is disadvantageous for the printability of PLA/CNT filaments.

3.1.2. Effects of the CNT content on the rheological properties

Fig. 2 shows the effects of the CNT content on the MFR of PLA/CNT blends. The MFR of the PLA/CNT composites decreased with increasing CNT content. The MFR value of PLA was 29.38 g/10 min, whereas that of PLA/CNT blends containing 8 wt% CNT was 6.91 g/10 min. This measurement clearly shows that the flow properties of PLA can be reduced by the addition of CNT. The decline of the MFR was a result of the nucleation effect between PLA and CNT, which enhances the intermolecular forces and increases the activation energy required for viscous flow. Acting as a plunger at the feed charge door of the FDM equipment, the filament extrudes the fused polymer out of the nozzle in the FDM process. A greater MFR value is beneficial to the improvement of fabrication efficiency and forming quality for FDM [18]. More stringent demands were put forward with the reduction of the MFR for

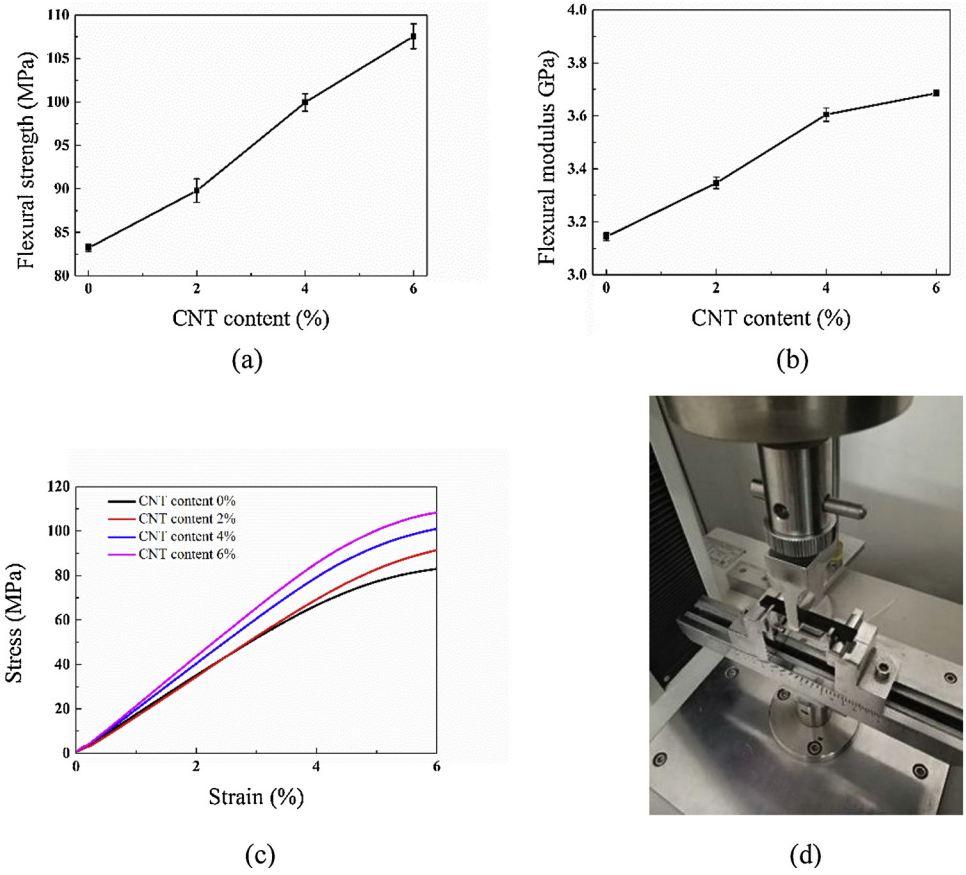

Fig. 5. Effects of the CNT content on the (a) flexural strength, (b) flexural modulus, and (c) representative stress-strain curves and (d) flexural test diagram.

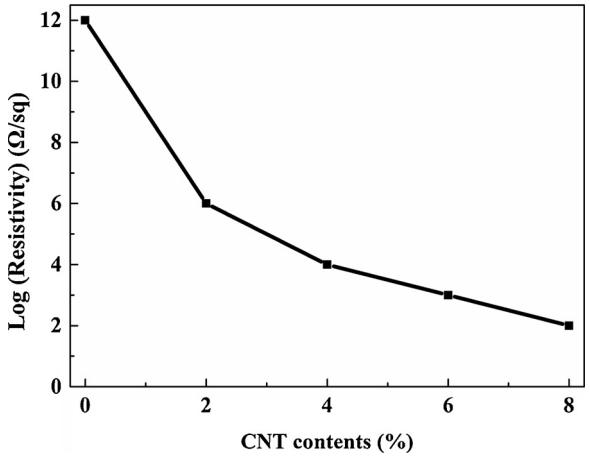

Fig. 6. Effects of the CNT content on the electrical resistivity.

the FDM process in practical application. In fact, continuous and reliable printing can be achieved when the content of carbon nanotubes is less than or equal to 6 wt%. Only the specimens of electrical resistivity testing can be printed using 8 wt% PLA/CNT filament, while the tensile and flexural specimens cannot be guaranteed to be well formed.

3.2. Mechanical properties

3.2.1. Effects of the CNT content on the tensile results

As shown in Fig. 3, the tensile results of PLA/CNT blends with different CNT content demonstrate that the tensile strength and elastic modulus increased with increasing CNT content. The tensile strength of the composite increased by 64.12% by adding 6 wt% CNT compared with that of pure PLA. The same phenomena can be found in the previous researches [24,25]. CNT could be effectively employed as reinforcers in polymer composites based on well-distributed nanoparticles, which can provide good dispersion of CNT in the PLA matrix and improve interface strengthening. Accordingly, the force applied upon the PLA/CNT may be effectually transferred to the CNT, resulting in a significant increase in the tensile strength and elastic modulus of the PLA/CNT-printed parts. Based on the covalent interactions, extensive graft polymerization occurred to improve the adhesive force between the PLA and CNT [23]. It can be clearly seen from the SEM micrographs in Fig. 4 that the interfacial adhesion is better and that the layer-by-layer effect becomes weaker with the addition of CNT. Fig. 3(c) shows representative tensile strain-stress curves of test pieces with different CNT contents.

3.2.2. Effects of the CNT content on the flexural results

The flexural strength and flexural modulus of PLA/CNT composites with different CNT contents are shown in Fig. 5(a) and (b), respectively. The results illustrate that the flexural strength and flexural modulus increased with increasing CNT content. The addition of 6 wt% CNT promoted a 29.29% increase in the flexural strength and a 17.39% increase in the flexural modulus of the composites compared with pure PLA. The mixture of PLA and CNT increased the proportion of the continuous phase and thereby increased the flexural strength. Moreover, the adherence between the layers was also conducive to increasing the flexural strength of the PLA/CNT blends [18]. Typical flexural strain-stress curves of all the samples with different CNT contents are shown in Fig. 5(c).

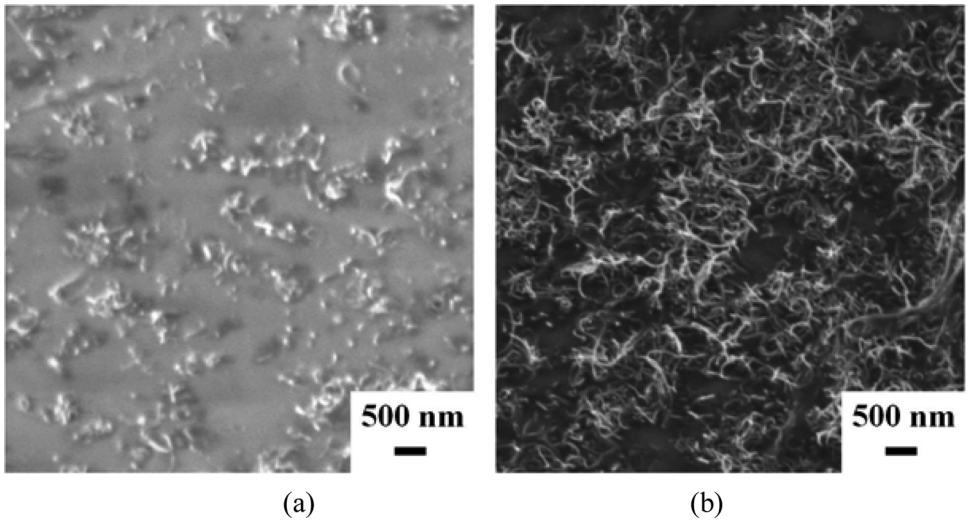

Fig. 7. The SEM micrographs of electrical resistivity samples with (a) 4 wt% and (b) 8 wt% CNT content.

Table 4
Experimental scheme and results.

Exp. No.	Factors			Response
	A / mm/s	B / mm	C / ℃	Electrical resistivity / Ω/sq
1	60	215	0.1	98.3
2	40	215	0.2	39.7
3	60	200	0.2	60.1
4	20	215	0.1	71.4
5	40	215	0.2	37.6
6	40	230	0.1	65.8
7	20	215	0.3	18.2
8	20	230	0.2	21.5
9	20	200	0.2	40.9
10	40	200	0.1	113.4
11	40	215	0.2	37.8
12	40	215	0.2	40.5
13	60	230	0.2	31.3
14	60	215	0.3	21.5
15	40	230	0.3	14.9
16	40	200	0.3	19.7
17	40	215	0.2	35.3

Table 5
The ANOVA for electrical resistivity.

Source	SS	DF	MS	F-Value	P-Value	Remarks
Model	12,653.44	9	1405.94	216.31	< 0.0001	Significant
A	438.08	1	438.08	67.40	< 0.0001	Significant
B	1265.05	1	1265.05	194.63	< 0.0001	Significant
C	9425.65	1	9425.65	1450.16	< 0.0001	Significant
A^2	0.73	1	0.73	0.11	0.7482	
B^2	1.98	1	1.98	0.30	0.5986	
C^2	895.67	1	895.67	137.80	< 0.0001	Significant
AB	22.09	1	22.09	3.40	0.1078	
AC	139.24	1	139.24	21.42	0.0024	Significant
BC	457.96	1	457.96	70.46	< 0.0001	Significant
Residual	45.50	7	6.50			
Lack of Fit	29.03	3	9.68	2.35	0.2136	
Total	12,698.94	16				

3.3. Electrical conductivity

3.3.1. Effects of the CNT content on the electrical resistivity

Fig. 6 shows the specific resistivity of PLA with different CNT contents. The original electrical resistivity of PLA is 1×10^{12} Ω/m^2. When the CNT content increases from 0% to 2%, the electrical resistivity reduces from 1×10^{12} to 1×10^{6} Ω/m^2. With the addition of 8 wt% CNT, the electrical resistivity reduces to as low as 1×10^{2} Ω/m^2. This phenomenon indicates that the increase of CNT content in PLA/CNT can promote the formation of permeable conduction paths and distribution of charge on the surface of the composites because of the excellent electrical conductivity of the CNT, as shown in Fig. 7. Therefore, a higher proportion of CNT can bring excellent conductivity suitable for industrial FDM filament preparation. The results are consistent with previous reports [3,17,26].

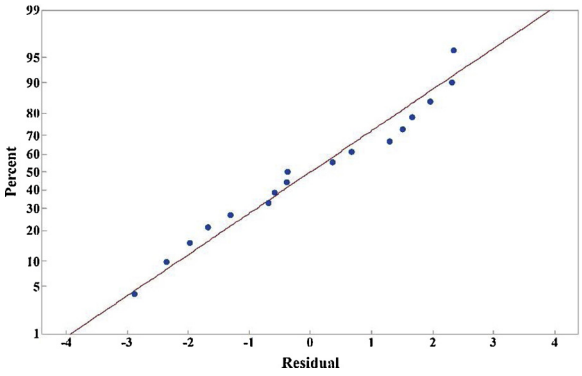

Fig. 8. Normal probability plot of the residuals for resistivity.

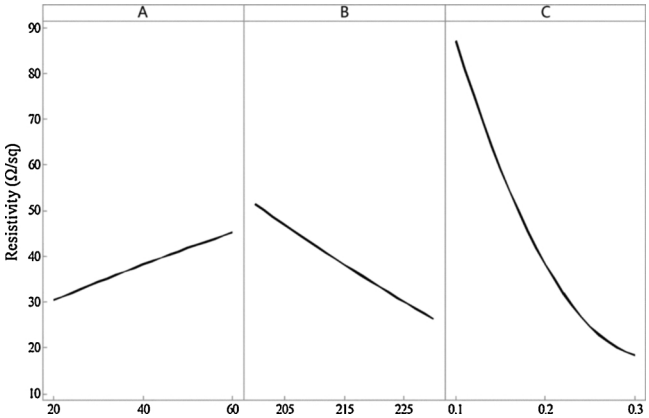

Fig. 9. Main effect plots showing the effect of processing parameters on the resistivity.

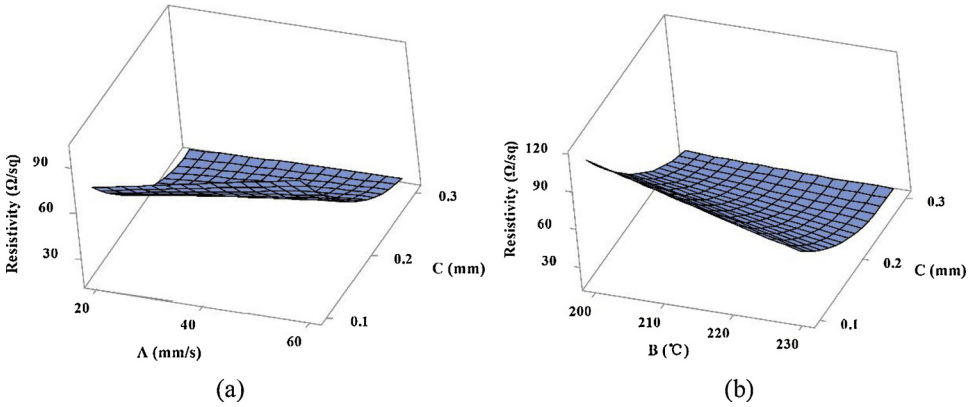

Fig. 10. Three-dimensional response surfaces of the (a) filling velocity and layer thickness and (b) liquefier temperature and layer thickness.

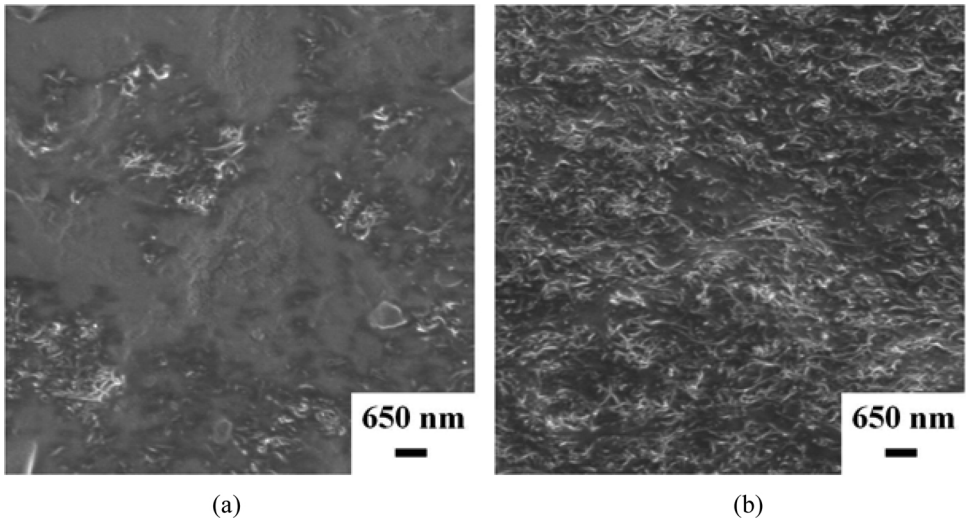

Fig. 11. The SEM micrographs of electrical resistivity samples obtained from a (a) high filling velocity (60 mm/s, specimen 3) and (b) low filling velocity (20 mm/s, specimen 9).

3.3.2. Effects of the process parameters on the electrical resistivity

As a kind of modeling method of experience, RSM is employed to investigate the interconnections of technological parameters and can accurately express the entire process. For investigating the effect of technological variables on electrical resistivity, experiments were carried out based on the Box-Behnken design (BBD). The concrete experimental schemes and results are acquired from each experimental run as illustrated in Table 4.

ANOVA is adopted to estimate the applicability of this model and assess to the significance of various factors to the response. The analysis of variance results of electrical resistivity are shown in Table 5. The P-value of the model is less than 0.0001, which represents a satisfactory fit of the created mathematical models.

Fig. 8 shows the normal probability plot of the residuals for the response of electrical resistivity. A linear distribution of points means that the results have no large deviations. Moreover, the model predictive capability is usually evaluated by the predicted R^2 value, and the value R^2 of 0.9964 indicates that this relatively accurate prediction model can be extensively employed experimentally in further researches.

Fig. 9 presents the main effect plots of three process parameters on the resistivity. From this figure, it can be seen that the resistivity increases as the filling velocity increases, while it decreases as the liquefier temperature and layer thickness increase. Fig. 10 shows the three-dimensional response surfaces for the resistivity. It can be concluded from these graphs that increasing the filling velocity has a negative effect on the conductivity of the PLA/CNT composites. As shown in Fig. 11, a low filling velocity is more favorable for the uniform distribution of CNT than a high filling velocity. The same variation was found in a previous study [27]. The electrical resistance increases as the take-up velocity increases from 20 m/min to 100 m/min, which is very similar to the case of the filling velocity. Unlike the filling velocity, increasing the liquefier temperature has a positive effect on the electrical conductivity, which means that higher temperatures contribute to the excellent dispersion of CNT in the composites. Lin et al. [28] prepared PLA/CNT composites by melt blending and additional hot-press processing to achieve an improvement in the conductive properties. In addition, higher temperatures are beneficial to promoting adhesion between layers. It can be concluded from the SEM micrographs in Fig. 12 that with increasing liquefier temperature, higher bonding quality can be achieved between the layers. The favorable dispersion and the high interface bonding strength are conducive to enhancing the electrical conductivity of the printed parts [16]. It is disadvantageous for the aim of improving the electrical conductivity that incomplete adhesion occurs between layers when the liquefier temperature is 200°C, as shown in Fig. 12(a). Nevertheless, the influence of the layer thickness is much more obvious in the case of the resistivity than in the case of the other process parameters. More layers are needed to fabricate the same part when a thinner layer thickness is chosen, which has a detrimental effect on the electrical conductivity, as shown in Fig. 13. To achieve the target of minimal resistivity, a lower filling velocity, higher liquefier temperature and greater layer thickness should be selected

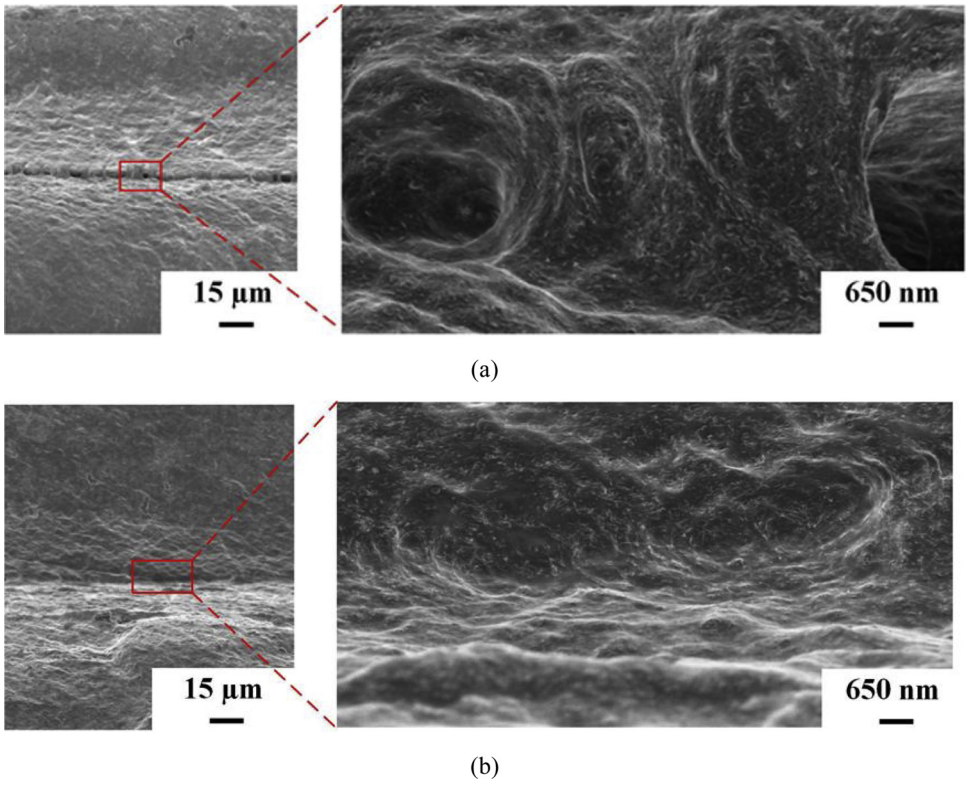

Fig. 12. The SEM micrographs of electrical resistivity samples obtained from a (a) low liquefier temperature (200℃, specimen 3) and (b) high liquefier temperature (230℃, specimen 13).

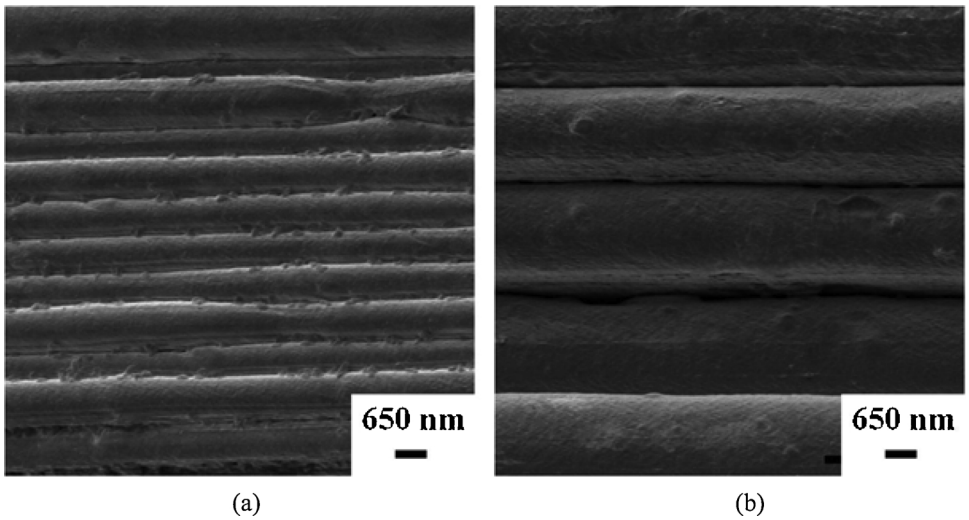

Fig. 13. The SEM micrographs of electrical resistivity samples obtained with a (a) low layer thickness (0.1 mm, specimen 4) and (b) high layer thickness (0.3 mm, specimen 7).

when conditions permit.

4. Summary and conclusion

In this study, filaments based on PLA/CNT matrices were prepared for the FDM process. The results demonstrate that the CNT content has a significant influence on the mechanical properties and conductivity properties. The conclusions obtained from the present work are listed below:

1) The flow properties, crystallization and melting behavior of PLA can be degraded by the addition of CNT, which is disadvantageous to the FDM process.
2) The addition of 6 wt% CNT results in a 64.12% increase in tensile strength and a 29.29% increase in flexural strength of the blend in comparison to pure PLA. In addition, the electrical resistivity varies from approximately 1×10^{12} Ω/sq to 1×10^{2} Ω/sq among the different CNT contents from 0 wt% to 8 wt%.
3) This paper assesses the effect of the filling velocity, liquefier temperature and layer thickness on the electrical resistivity. A lower filling velocity, higher liquefier temperature and greater layer thickness should be selected to achieve excellent electrical conductivity. All of the above results demonstrate that PLA/CNT filaments are a promising functionalizing material for FDM.

Acknowledgments

The authors wish to acknowledge the financial support from the National Natural Science Foundation of China (grant No.51575442) and the National Natural Science Foundation of Shaanxi Province (grant No.2016JZ011).

References

[1] S. Ford, M. Despeisse, Additive manufacturing and sustainability: an exploratory study of the advantages and challenges, J. Clean. Prod. 137 (2016) 1573–1587.
[2] O.A. Mohamed, S.H. Masood, J.L. Bhowmik, M. Nikzad, J. Azadmanjiri, Effect of process parameters on dynamic mechanical performance of FDM PC/ABS printed parts through design of experiment, J. Mater. Eng. Perform. 25 (7) (2016) 2922–2935.
[3] W.W. Yu, J. Zhang, J.R. Wu, X.Z. Wang, Y.H. Deng, Incorporation of graphitic nano-filler and poly(lactic acid) in fused deposition modeling, J. Appl. Polym. Sci. 134 (15) (2017).
[4] A.K. Sood, R.K. Ohdar, S.S. Mahapatra, Parametric appraisal of mechanical property of fused deposition modelling processed parts, Mater. Des. 31 (1) (2010) 287–295.
[5] F. Rayegani, G.C. Onwubolu, Fused deposition modelling (FDM) process parameter prediction and optimization using group method for data handling (GMDH) and differential evolution (DE), Int. J. Adv. Manuf. Technol. 73 (1-4) (2014) 509–519.
[6] A. Peng, X. Xiao, R. Yue, Process parameter optimization for fused deposition modeling using response surface methodology combined with fuzzy inference system, Int. J. Adv. Manuf. Technol. 73 (1-4) (2014) 87–100.
[7] M. Dawoud, I. Taha, S.J. Ebeid, Mechanical behaviour of ABS: an experimental study using FDM and injection moulding techniques, J. Manuf. Process. 21 (2016) 39–45.
[8] A.P. Gordon, J. Torres, M. Cole, A. Owji, Z. DeMastry, An approach for mechanical property optimization of fused deposition modeling with polylactic acid via design of experiments, Rapid Prototyp. J. 22 (2) (2016) 387–404.
[9] B.N. Panda, K. Shankhwar, A. Garg, J. Zhang, Performance evaluation of warping characteristic of fused deposition modelling process, Int. J. Adv. Manuf. Technol. 88 (5-8) (2016) 1–13.
[10] R. Singh, S. Singh, K. Mankotia, Development of ABS based wire as feedstock filament of FDM for industrial applications, Rapid Prototyp. J. 22 (2) (2016) 300–310.
[11] O.A. Mohamed, S.H. Masood, J.L. Bhowmik, Mathematical modeling and FDM process parameters optimization using response surface methodology based on Q-optimal design, Appl. Math. Model. 40 (23-24) (2016) 10052–10073.
[12] E. Vahabli, S. Rahmati, Application of an RBF neural network for FDM parts' surface roughness prediction for enhancing surface quality, Int. J. Precis. Eng. Manuf. Technol. 17 (12) (2016) 1589–1603.
[13] Y. Jia, H. He, X. Peng, S. Meng, J. Chen, Y. Geng, Preparation of a new filament based on polyamide-6 for three-dimensional printing, Polym. Eng. Sci. 57 (12) (2017).
[14] F. Ning, W. Cong, J. Qiu, J. Wei, S. Wang, Additive manufacturing of carbon fiber reinforced thermoplastic composites using fused deposition modeling, Compos. Part B-Eng. 80 (2015) 369–378.
[15] Q. Chen, J.D. Mangadlao, J. Wallat, A.D. Leon, J.K. Pokorski, R.C. Advincula, 3D printing biocompatible polyurethane/poly(lactic acid)/graphene oxide nanocomposites: anisotropic properties, ACS Appl. Mater. Interface 9 (4) (2017) 4015.
[16] D. Zhang, B. Chi, B. Li, Z. Gao, Y. Du, J. Guo, et al., Fabrication of highly conductive graphene flexible circuits by 3D printing, Synth. Met. 217 (2016) 79–86.
[17] G. Postiglione, G. Natale, G. Griffini, M. Levi, S. Turri, Conductive 3D microstructures by direct 3D printing of polymer/carbon nanotube nanocomposites via, liquid deposition modeling, Compos. Part A-Appl. 76 (2015) 110–114.
[18] J. Zhu, Y. Hu, Y. Tang, B. Wang, Effects of styrene–acrylonitrile contents on the properties of ABS/SAN blends for fused deposition modeling, J. Appl. Polym. Sci. 134 (7) (2016).
[19] X. Tian, T. Liu, C. Yang, Q. Wang, D. Li, Interface and performance of 3D printed continuous carbon fiber reinforced PLA composites, Compos. Part A-Appl. 88 (2016) 198–205.
[20] J. Wang, H. Xie, L. Wang, T. Senthil, R. Wang, Y. Zheng, Anti-gravitational 3D printing of polycaprolactone-bonded Nd-Fe-B based on fused deposition modeling, J. Alloys. Compd. 715 (2017) 146–153.
[21] A. Dorigato, V. Moretti, S. Dul, S.H. Unterberger, A. Pegoretti, Electrically conductive nanocomposites for fused deposition modelling, Synth. Met. 226 (2017) 7–14.
[22] S. Barrau, C. Vanmansart, M. Moreau, A. Addad, G. Stoclet, J.M. Lefebvre, et al., Crystallization behavior of carbon nanotube − polylactide nanocomposites, Macromolecules 44 (16) (2011) 6496–6502.
[23] K. Chrissafis, K.M. Paraskevopoulos, A. Jannakoudakis, T. Beslikas, D. Bikiaris, Oxidized multiwalled carbon nanotubes as effective reinforcement and thermal stability agents of poly(lactic acid) ligaments, J. Appl. Polym. Sci. 118 (5) (2010) 2712–2721.
[24] T.Y. Jin, Y.G. Jeong, C.L. Sang, G.M. Byung, Influences of poly(lactic acid)-grafted carbon nanotube on thermal, mechanical, and electrical properties of poly(lactic acid), Polym. Adv. Technol. 20 (7) (2010) 631–638.
[25] G. Gorrasi, A. Sorrentino, Photo-oxidative stabilization of carbon nanotubes on polylactic acid, Polym. Degrad. Stabil. 98 (5) (2013) 963–971.
[26] S. Shao, S. Zhou, L. Li, J. Li, C. Luo, J. Wang, et al., Osteoblast function on electrically conductive electrospun PLA/MWCNTs nanofibers, Biomaterials 32 (11) (2011) 2821–2833.
[27] P. Pötschke, T. Andres, T. Villmow, S. Pegel, H. Brünig, K. Kobashi, et al., Liquid sensing properties of fibres prepared by melt spinning from poly(lactic acid) containing multi-walled carbon nanotubes, Compos. Sci. Technol. 70 (2) (2010) 343–349.
[28] W.Y. Lin, Y.F. Shih, C.H. Lin, C.C. Lee, Y.H. Yu, The preparation of multi-walled carbon nanotube/poly(lactic acid) composites with excellent conductivity, J. Taiwan Inst. Chem. E 44 (3) (2013) 489–496.